On two site-specific nitrite-sensing nanocomposites having a core-shell structure: Construction, characterization and sensing performance

Muhetaer Kadeerhazi [a], Azam Ali [b], Alaa El-Din Bekhit [c,*]

[a] College of Food Science and Pharmacy, Xinjiang Agricultural University, Urumqi 830052, China
[b] Department of Applied Science, University of Otago, Dunedin 9054, New Zealand
[c] Department of Food Science, University of Otago, Dunedin 9054, New Zealand

ARTICLE INFO

ABSTRACT

This paper reported two site-specific nitrite-sensing nanocomposite samples having a core-shell structure, where Fe_3O_4 nanoparticles were used as core, two rhodamine derivatives served as chemosensor and MCM-41 was applied as supporting host, respectively. These composite samples and their structure were analyzed and confirmed SEM/TEM, XRD, N_2 adsorption/desorption, magnetic feature, IR and thermogravimetric analysis. Their nitrite sensing performance was discussed based on emission quenching, with limit of detection as low as 1.2 μM. Detailed analysis suggested that these composite samples followed a static sensing mechanism based on an additive reaction between NO^+ and chemosensors. After being quenched by nitrite, these samples could be recovered by sulphamic acid.

© 2016 Elsevier B.V. All rights reserved.

1. Introduction

As a class of widely-used antistaling agent, nitrite salts have been considered as important analytical targets since they react with amines of living body and release carcinogenic nitrosamines, increasing cancer risks and deformities [1–3]. The World Health Organization (WHO) has consequently set a ceiling limit in drinking water for nitrite as 65 μM [4]. Modern analytical techniques have been proved valid and practicable for nitrite sensing, such as spectrofluorimetry, electrometry, capillary electrophoresis and chromatography. Their precise readings, however, are based on fine equipment and complicated pretreatment procedures, which makes them improper for on-line monitoring and in-field detection [5–9].

Optical sensing technique has been frequently nominated as a candidate owing to its virtues of simple equipment, non-invasive character and easy operation. In addition, optical signals are suitable for long-distance monitoring since they are immune from electromagnetic interference [10]. Various fluorescent dyes and sensitizers have been developed as nitrite sensing chemosensors, such as rhodamine, coumarin, fluorescein, assafranine and their derivatives [11–15]. For example, a carbazole-based chemosensor finishes its recognition through a reaction between nitrite and I^- ion [12]. Similarly, rhodamine derivatives form a nitroso compound in acid medium with nitrite [14]. To guarantee fluent analyte diffusion and sensing, supporting host is usually applied to immobilize chemosensor molecules, including polymers, silicates, metal oxides and so on [16–18]. Among these candidates, a mesoporous

silica molecular sieve MCM-41 has emerged as a promising one by showing large surface-area-to-volume ratio, high stability, chemical inertness and highly ordered tunnels.

Except for a promising supporting host and a shining chemosensor, there is still another important function to be met, which is recyclability. This function requires site-specific performance from corresponding sensing system after it finishes its recognition. To satisfy this objective, multifunctional composite materials have been proposed since they generally combine features of each component and preserve them well [19,20]. As a class of frequently mentioned site-specific materials, magnetic composite ones, such as Fe_3O_4 based ones, have shown their application in magnetic guiding, sample sorting and isolating [21–23]. In addition, these magnetic composite materials can be readily modified, such as silica coating, to minimize magnetic effect on chemosensor emission and connect additional components [24–25].

Guided by above consideration, in this effort, two site-specific nitrite-sensing nanocomposite samples having a core-shell structure have been designed, where Fe_3O_4 nanoparticles are used as core, two rhodamine derivatives serve as chemosensor and MCM-41 is applied as supporting host, respectively. Their identification and nitrite sensing performance are discussed in detail.

2. Experimental details

Scheme 1 shows preparation strategy for our desired nitrite sensing nanocomposite samples, RB@MCM-41@Fe_3O_4 and RSB@MCM-41@Fe_3O_4. Detailed synthesis for supporting matrix MCM-41@Fe_3O_4 and chemosensors is given as Supporting information. A general preparation route for RB@MCM-41@Fe_3O_4 and RSB@MCM-41@Fe_3O_4 is described as

* Corresponding author.
E-mail address: BekhitAED071@163.com (A.E.-D. Bekhit).
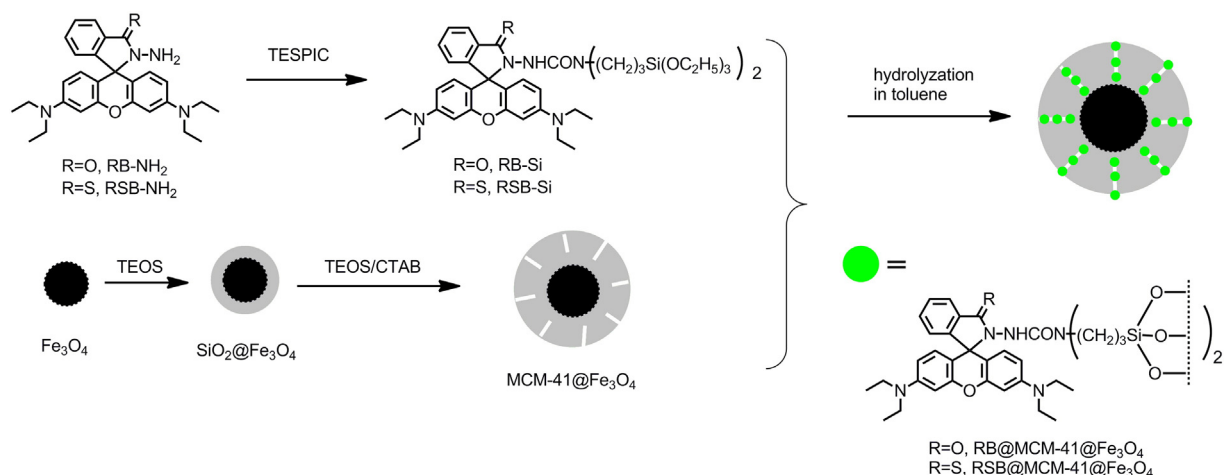
Scheme 1. Preparation strategy for RB@MCM-41@Fe$_3$O$_4$ and RSB@MCM-41@Fe$_3$O$_4$.

follows. The mixture of MCM-41@Fe$_3$O$_4$ (1 g) and RB-Si (or RSB-Si, 0.8 g, excess) in anhydrous toluene (50 mL) was heated at 120 °C for 12 h under N$_2$ protection. After cooling, solid product was collected and washed with toluene and ethanol to give RB@MCM-41@Fe$_3$O$_4$ (or RSB@MCM-41@Fe$_3$O$_4$).

3. Results and discussion

3.1. Design strategy and morphology of RB@MCM-41@Fe$_3$O$_4$ and RSB@MCM-41@Fe$_3$O$_4$

For a clear understanding on these two nitrite sensing nanocomposite samples, their design strategy is explained as follows. Recyclability is desired from these nitrite sensing samples, which asks a site-specific ability after they accomplish nitrite recognition. To satisfy this objective, Fe$_3$O$_4$ magnetic core in RB@MCM-41@Fe$_3$O$_4$ and RSB@MCM-41@Fe$_3$O$_4$ is designed for magnetic guiding. To decrease magnetic aggregation, facilitate following functionalization procedures and minimize magnetic effect on chemosensor emission, Fe$_3$O$_4$ magnetic core is encapsulated by amorphous silica. Owing to its high surface-area-to-volume ratio and highly regular hexagonal tunnels, silica molecular sieve MCM-41 has been proved as a promising supporting host for optical dopants [10,26,27]. In this work, MCM-41 is chosen as supporting host for our two chemosensors since its regular tunnels are positive for analyte adsorption and diffusion. Our two chemosensors are covalently embedded into MCM-41 host to minimize chemosensor leakage and improve their stability. Given above assumption, good nitrite sensing performance with recyclability is desired from RB@MCM-41@Fe$_3$O$_4$ and RSB@MCM-41@Fe$_3$O$_4$.

For a visual evaluation on these composite samples, scanning electron microscopy (SEM) images of bare Fe$_3$O$_4$ nanoparticles, SiO$_2$@Fe$_3$O$_4$, MCM-41@Fe$_3$O$_4$, RB@MCM-41@Fe$_3$O$_4$ and RSB@MCM-41@Fe$_3$O$_4$ are shown in Fig. 1. Our as-synthesized Fe$_3$O$_4$ nanoparticles are generally spherical ones with mean diameter of ~360 nm. These nanoparticles are aggregated together owing to their magnetic nature, showing rough surface and bad dispersal. Amorphous silica encapsulation increases their mean diameter to ~400 nm (SiO$_2$@Fe$_3$O$_4$), with their surface greatly smoothed. Their dispersal is obviously improved as well, which means that SiO$_2$ layer (20 nm) is effective on blocking magnetic aggregation. MCM-41 tunnels are constructed onto SiO$_2$@Fe$_3$O$_4$, so MCM-41@Fe$_3$O$_4$ diameter is further increased to 500 nm. After co-hydrolyzation and chemosensor loading, good monodispersal is observed for RB@MCM-41@Fe$_3$O$_4$ and RSB@MCM-41@Fe$_3$O$_4$, which means that magnetic attraction has been successfully sealed in them. Their mean diameters are all round 500 nm, suggesting that these procedures have slim effect on particle diameter. It is thus assumed that our

chemosensors have been grafted into MCM-41 tunnels instead of sample surface, which will be further confirmed below. Tunnel length in RB@MCM-41@Fe$_3$O$_4$ and RSB@MCM-41@Fe$_3$O$_4$ is estimated as ~50 nm, which is consistent with their transmission electron microscopy (TEM) images shown in Fig. 1. Their core-shell structure is thus finally confirmed.

3.2. XRD analysis, N$_2$ adsorption/desorption and magnetic feature

For a fast analysis on the magnetic core in our composite samples, Fig. S1A (Supporting information) shows wide angle XRD (WAXRD) curves of bare Fe$_3$O$_4$ nanoparticles, MCM-41@Fe$_3$O$_4$, RB@MCM-41@Fe$_3$O$_4$ and RSB@MCM-41@Fe$_3$O$_4$. These four samples have nearly identical diffraction peaks which are quite similar to those of standard Fe$_3$O$_4$ nanoparticles [19,20,26,27]. This result confirms that Fe$_3$O$_4$ core has been prepared successfully and well preserved after silica encapsulation, MCM-41 construction and chemosensor loading procedures. Their different diffraction intensity values should be attributed to above modification procedures which actually decrease Fe$_3$O$_4$ weight ratio and regularity in these samples. Small angle XRD (SAXRD) patterns of MCM-41@Fe$_3$O$_4$, RB@MCM-41@Fe$_3$O$_4$ and RSB@MCM-41@Fe$_3$O$_4$ are shown in Fig. S1B (Supporting information) so that their mesoporous structure can be revealed. Similar to literature reports, three well-resolved diffraction peaks are detected for each SAXRD curve, labeled as d_{100}, d_{110} and d_{200}, respectively [10]. This result suggests that there is mesoporous structure on MCM-41@Fe$_3$O$_4$ which has been well preserved after chemosensor loading procedure.

Aiming at a further understanding on the mesoporous structure on sample surface, N$_2$ adsorption/desorption isotherms of MCM-41@Fe$_3$O$_4$, RB@MCM-41@Fe$_3$O$_4$ and RSB@MCM-41@Fe$_3$O$_4$ are recorded and shown in Fig. S2 (Supporting information). Regardless of their different adsorption volumes, type-IV isotherms are observed for all four samples which are much similar to those of standard MCM-41 samples [10]. This observation finally confirms that MCM-41 tunnels have been successfully prepared onto Fe$_3$O$_4$ core and well preserved after chemosensor loading procedure. Efficient analyte adsorption and fluent analyte transportation are expected from these highly ordered MCM-41 tunnels [10]. As for MCM-41@Fe$_3$O$_4$, its surface area, pore volume and pore size are measured as 636.237 m$^2 \cdot$g^{-1}, 0.566 cm$^3 \cdot$g^{-1} and 2.646 nm, respectively. After chemosensor loading procedure, these parameters are measured as 441.185 m$^2 \cdot$g^{-1}, 0.442 cm$^3 \cdot$g^{-1} and 2.420 nm for RB@MCM-41@Fe$_3$O$_4$, 411.335 m$^2 \cdot$g^{-1}, 0.406 cm$^3 \cdot$g^{-1} and 2.315 nm for RSB@MCM-41@Fe$_3$O$_4$, respectively. It is clear that mesoporous parameters of RB@MCM-41@Fe$_3$O$_4$ and RSB@MCM-41@Fe$_3$O$_4$ are smaller than those of MCM-41@Fe$_3$O$_4$. Combined with their similar diameters to that of MCM-41@Fe$_3$O$_4$, we come to a conclusion